IEEE Access
Multidisciplinary ⋮ Rapid Review ⋮ Open Access Journal

Received 8 August 2023, accepted 31 August 2023, date of publication 6 September 2023, date of current version 12 September 2023.

Digital Object Identifier 10.1109/ACCESS.2023.3312573

RESEARCH ARTICLE

Multi-Objective Optimization Scheduling of Active Distribution Network Considering Large-Scale Electric Vehicles Based on NSGAII-NDAX Algorithm

JINGWEN CHEN[1], LEI MAO[1], YAOXIAN LIU[1], JINFENG WANG[2], AND XIAOCHEN SUN[2]
[1]College of Electrical and Control Engineering, Shaanxi University of Science and Technology, Xi'an 710021, China
[2]State Grid Shaanxi Electric Power Company Ltd. Research Institute, Xi'an 710065, China

Corresponding author: Lei Mao (sust_mlml@163.com)

This work was supported in part by the Key Research and Development Plan of Shaanxi Province under Grant 2023-YBGY-304, and in part by the State Grid Shaanxi Electric Power Company Ltd. Science and Technology Project "Research on optimal allocation and comprehensive value measurement of user-side energy storage capacity for new power system" under Grant 5226JY230008.

ABSTRACT With the rapid growth of electric vehicle (EV) ownership, the problem of increased peak loads on distribution networks due to large-scale EV integration needs to be addressed. This study proposes an active distribution network multi-objective optimization scheduling method. It takes into account the charging demands of large-scale EVs and aims to minimize distribution network operating costs, reduce net load variance, and maximize the photovoltaic (PV) consumption rate. First, the Monte Carlo sampling method is used to analyze the charging load demands of a large number of EVs. Next, we construct a multi-objective optimization scheduling model for the active distribution network. This model integrates the charging demands of EVs with the operating constraints of the distribution network. To tackle the multi-objective optimization problem, we propose the NSGAII-NDAX algorithm. Additionally, we employ a fuzzy theory-based method to select the Pareto optimal solution set, addressing the challenge of decision-making complexity posed by the large size and information-rich content of the optimal solution set. Finally, the effectiveness of the proposed method in the comparative analysis of multiple scenarios is verified by an improved IEEE 33-node example. The experimental results show that the proposed model and method can effectively utilize EV charging load optimization to reduce the peak-to-valley difference in the system load while ensuring the system's economic operation and the maximum PV consumption rate. Compared with the other algorithms, the NSGAII-NDAX algorithm has stronger optimization ability and can better handle multi-objective optimization problems.

INDEX TERMS Electric vehicle, active distribution network, multi-objective optimization, NSGAII-NDAX algorithm, fuzzy theory.

I. INTRODUCTION

Due to the transportation sector's excessive reliance on fossil fuels, has resulted in severe air pollution and greenhouse gas emissions, leading to significant environmental problems [1]. As governments and environmental advocates prioritize environmental protection and sustainable development, there is a challenging objective to integrate large-scale EVs into modern power grids, enabling the establishment, design, and management of clean, efficient, low-carbon, and sustainable energy systems [2].

The significant rise in charging loads of EVs has had a considerable impact on the overall load of the power system, The industry recognizes the critical importance of managing EV charging loads. The power demand from the large-scale deployment of EVs may surpass the grid's capacity, resulting

The associate editor coordinating the review of this manuscript and approving it for publication was Cong Pu.

in potential issues for power system operators due to uncoordinated charging [3], [4]. Additionally, the integration of a large number of EVs into the grid contributes significantly to power losses [5], [6]. Strategies such as implementing uniform charging, intelligent metering, and optimizing the siting and sizing of charging stations, can help reduce energy losses [7], [8]. However, the extensive integration of large-scale EVs with the grid can lead to transformer overheating, causing both economic and safety issues [9], [10]. Therefore, as EVs become more prevalent, the power system needs to overcome various challenges in integrating them on a large scale [11]. One of the primary challenges is how to effectively manage and schedule the charging loads of EVs to ensure the stability, reliability, and cost-effectiveness of the power system.

A significant amount of research has been conducted to address the negative impacts of EV charging on the power grid. Various controlled charging strategies have been proposed, including time-of-use pricing-based control, dynamic programming, and sequential quadratic programming, among others. It is crucial to implement appropriate scheduling strategies to mitigate the fluctuations caused by EVs, ensuring the safe and stable operation of the power grid [12]. Reference [13] studies have investigated the effects of large-scale EVs and high-penetration renewable energy sources on the power system. In related work, the concept of aggregators was introduced as intermediaries between end-users and distributed renewable energy systems, enabling ancillary services through load response [14]. Experimental results have demonstrated that optimized scheduling of EVs and renewable energy sources can effectively mitigate the adverse impacts of large-scale EVs charging load and renewable energy generation uncertainty on the power system.

In [15], an optimization model is established to minimize the peak-valley difference. The charging time for users is optimized using a genetic algorithm. Similarly, [16] proposes an ordered charging scheduling strategy specifically tailored to electric vehicle swapping stations, with a focus on controlling the charging power of these stations. Additionally, [17] presents an ordered charging method that relies on load forecasting and employs nonlinear optimization techniques to schedule the charging load, aiming to minimize the fluctuation of the overall load curve when integrating the charging load from electric vehicles.

Moreover, energy scheduling in microgrids that incorporate EVs and renewable energy was investigated in [18], where an optimization scheduling model considering the intermittent characteristics of renewable energy was established to minimize operational cost and power loss. Recent research has proposed an economic scheduling model based on information gap decision theory, considering demand response and coordinated EV charging, to address the multi-objective optimization scheduling problem of large-scale EV integration into active distribution networks [19]. Furthermore, an optimization scheduling model was developed [20], taking into account the high pollution and non-renewability of coal-fired generation, the clean and renewable nature of wind power, and the intermittent and fluctuating characteristics, while considering vehicle-to-grid (V2G) capabilities and generator operating costs. However, these studies have limitations, including singular optimization control objectives, limited scenarios, and insufficient consideration of constraints related to grid security and operation.

Therefore, there is a pressing need to address the problem of multi-objective optimization scheduling for the large-scale integration of electric vehicles into active distribution networks. This topic has gained significant attention in power system research due to its importance. Future research should focus on conducting in-depth investigations in this area. Moreover, Table 1 concludes the existing gaps and main contributions of this work.

TABLE 1. Comparison existing works and this work.

Reference	large-scale EVs	Safe constraint	Cost	PV consumption	Net load variance	Solution algorithm
[14]	✓	×	✓	✓	×	MILP
[15]	×	×	×	×	✓	GA
[16]	×	✓	×	×	✓	PSO
[17]	✓	×	✓	×	✓	Non-linear
[18]	✓	×	×	×	✓	CVX
[19]	✓	✓	✓	✓	×	CPLEX
[20]	×	✓	✓	×	×	CPLEX
Current work	✓	✓	✓	✓	✓	NGSAII-NDAX

This paper proposes an active distribution network multi-objective optimization scheduling method that addresses the issue of increased peak loads on distribution networks caused by the large-scale integration of EVs. The method is based on the charging demands of a large number of EVs and aims to balance the minimization of distribution network operating costs, net load curve variance, and maximization of the PV consumption rate. The main contributions are as follows:

1) A multi-objective optimization scheduling model is developed, incorporating factors such as system operating cost, photovoltaic consumption rate, and net load variance, while considering the constraints of electric vehicle charging demands and distribution grid security.

2) To address the limitations of the simulated binary crossover (SBX) operator in the NSGAII algorithm, a normal distribution adaptive crossover operator is introduced, and the NSGAII-NDAX algorithm is proposed to alleviate the problem of getting stuck in local optima.

3) The evaluation method combining NSGAII-NDAX algorithm and fuzzy theory is used to screen the Pareto

optimal solution set, which solves the challenge brought by the large scale and large amount of information of the optimal solution set. Additionally, a scheduling strategy considering the charging load of large-scale EVs is proposed. This paper provides an overview of the current research status on the integration of large-scale electric vehicles into active distribution networks. The remaining sections are organized as follows: Section II presents a comprehensive analysis of the charging demands of EVs, explores the key factors influencing EV charging loads, and investigates the impact of EVs of different scales on the distribution network. Section III aims to optimize the operational cost, reduce net load variance, and improve the PV integration rate in active distribution networks by establishing a multi-objective optimization scheduling model. Section IV proposed the NSGAII-NDAX algorithm, which incorporates a normal distribution adaptive crossover operator. Fuzzy theory is also applied to evaluate and select compromise scheduling solutions from the Pareto optimal solution set. Section V verifies the effectiveness of the proposed algorithm and scheduling scheme through simulation in the IEEE33-node active distribution network system. Different scenarios and algorithms are set for comparative study. Finally, Section VI drew the conclusion of the study based on the findings of the previous paper.

II. CALCULATION OF EV CHARGING LOAD

Accurately calculating the load required for EV charging is essential for the distribution network and forms the basis for analyzing the participation of EVs in system operation and scheduling. A variety of factors significantly impact EV charging loads, such as EV penetration rate, initial state of charge (SOC), charging power, battery capacity, and initial charging time [21]. In this study, we assume that EVs do not influence users' travel habits. Therefore, we simulate EVs' driving and charging behaviors based on the driving behavior of conventional fuel vehicles. Additionally, we take into account the probability distribution of all stochastic factors and employ Monte Carlo random sampling methods to simulate EV charging loads at various scales.

A. MONTE CARLO SAMPLING

The Monte Carlo method, also known as statistical simulation or random sampling technique, is a computational method based on probability and statistical theory. It associates the problem to be solved with a certain probability model and utilizes computer-based statistical simulation or sampling to obtain approximate solutions. While AI-based methods and their applicability in data generation and analysis show promise, the Monte Carlo simulation offers a computationally efficient approach with the ability to handle complex random processes and generate diverse charging load curves.

In the context of this study, the Monte Carlo simulation plays a crucial role in capturing the uncertainty and variability of real-world charging behaviors. It provides high computational efficiency, allowing for the processing of complex random processes and the generation of different charging load curves. By leveraging the power of statistical sampling, the Monte Carlo method enables the effective approximation of the desired solutions.

Moreover, the Monte Carlo simulation offers significant advantages in dealing with the inherent uncertainties and dynamics associated with electric vehicle charging. It allows for the generation of multiple scenarios, reflecting the variability and stochastic nature of charging behavior. This capability is particularly relevant in the research context of this paper, where understanding and addressing the uncertainties and dynamics of charging behavior are essential.

B. PROBABILITY DISTRIBUTION OF DAILY MILEAGE

Through an analysis of data from the Transportation National Household Travel Survey (NHTS) conducted by the U.S. Department of Transportation, 14% of household vehicles are not used in a day, 43.5% of the vehicles are driven within about 32km, and 83.7% of the vehicles are driven within about 97km. After normalizing the statistical data, the daily mileage is approximated as a log-normal distribution using the method of maximum likelihood estimation. The fitting result is shown in Figure 1. The daily mileage follows a log-normal distribution, and its probability density function is shown below:

$$f_{\mathrm{D}}(x) = \frac{1}{x\sigma_{\mathrm{D}}\sqrt{2\pi}} \exp\left[-\frac{(\ln x - \mu_{\mathrm{D}})^2}{2\sigma_{\mathrm{D}}^2}\right] \tag{1}$$

where, $f_{\mathrm{D}}(x)$ represents the probability density function of daily mileage; x is the value of the random input variable of the probability density function $f_{\mathrm{D}}(x)$; μ_{D} is the mean of the log-normal distribution; σ_{D} is the variance of the log-normal distribution. Based on the fitted results, the approximate parameters are obtained as follows: the mean $\mu_{\mathrm{D}} = 3.2$ and the variance $\sigma_{\mathrm{D}} = 0.88$. After obtaining the probability distribution of daily travel distance, assuming the energy consumption of the electric vehicle is 100 kilometers and the battery is fully charged at the beginning of the journey, we can calculate the probability distribution of the SOC of the electric vehicle at the end of the trip.

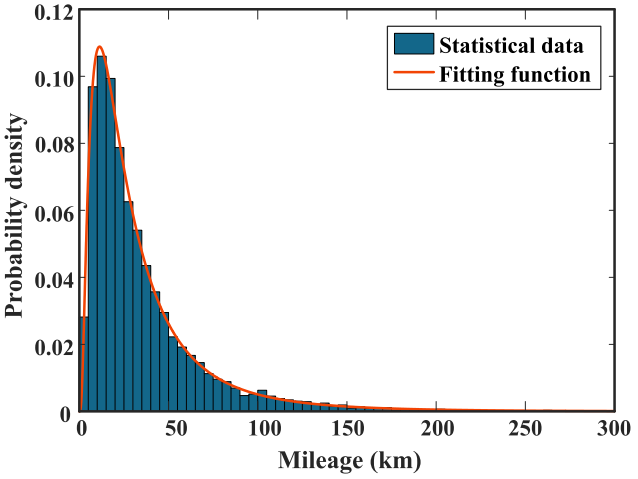

FIGURE 1. Probability distribution of daily miles traveled.

C. PROBABILITY DISTRIBUTION OF INITIAL CHARGING TIME

In the disordered charging mode, there is usually a certain correlation between the starting charging time and the time of the last return trip. According to statistical data from the NHTS, the distribution of starting charging times approximately follows a normal distribution. The fitting result is shown in Figure 2. Therefore, the probability density function of the normal distribution can be used to describe the initial charging time distribution characteristic, and its probability density function is shown below:

$$f_{\mathrm{I}}(x)=\begin{cases}\dfrac{1}{\sigma_{\mathrm{I}}\sqrt{2\pi}}\exp\left[-\dfrac{(x-\mu_{\mathrm{I}})^2}{2\sigma_{\mathrm{I}}^2}\right] & \mu_{\mathrm{I}}-12\le x\le 24\\ \dfrac{1}{\sigma_{\mathrm{I}}\sqrt{2\pi}}\exp\left[-\dfrac{(x+24-\mu_{\mathrm{I}})^2}{2\sigma_{\mathrm{I}}^2}\right] & 0\le x\le \mu_{\mathrm{I}}-12\end{cases} \tag{2}$$

where, $f_{\mathrm{I}}(x)$ represents the probability density function of initial charging time; x is the value of the random input variable of the probability density function $f_{\mathrm{I}}(x)$; μ_{I} is the mean of the normal distribution; σ_{I} is the variance of the normal distribution. Based on the fitted results, the approximate parameters are obtained as follows: the mean $\mu_{\mathrm{I}}=17.6$ and the variance $\sigma_{\mathrm{I}}=3.4$.

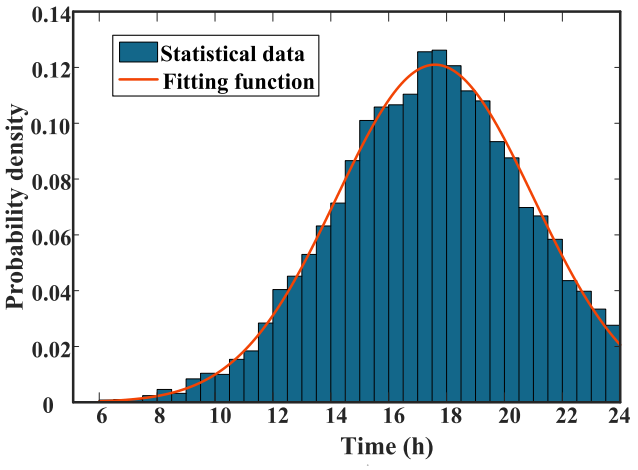

FIGURE 2. Probability distribution of initial charging time.

D. PROBABILITY DISTRIBUTION OF CHARGING POWER

During the standard low-speed charging process, the time taken for the charging initiation and termination stages is relatively negligible compared to the overall charging process [22]. Thus, for analytical purposes, these stages can be temporarily disregarded. Given the variability in charging characteristics among different types of EVs, and charging stations, the charging power can be approximated as a constant value. Assuming a uniform distribution within the range of 4-6 kW for the charging power, the probability density function can be expressed as follows:

$$f_{\mathrm{P}}(x)=\begin{cases}\dfrac{1}{2} & 4\le x\le 6\\ 0 & \text{other}\end{cases} \tag{3}$$

where, $f_{\mathrm{P}}(x)$ represents the probability density function of charging power.

E. PROBABILITY DISTRIBUTION OF BATTERY CAPACITY

Given the diversity and variability of battery suppliers utilized in electric vehicles, it is necessary to model the battery capacity of different EVs using probability distributions. In this case, the battery capacity values range from 20 to 30 kWh and follow a uniform distribution. Consequently, the probability density function that represents the distribution characteristics of the battery capacity can be expressed as follows:

$$f_{\mathrm{C}}(x)=\begin{cases}\dfrac{1}{10} & 20\le x\le 30\\ 0 & \text{other}\end{cases} \tag{4}$$

where, $f_{\mathrm{C}}(x)$ represents the probability density function of battery capacity.

F. CALCULATION OF EV CHARGING LOAD

Assuming that the charging time, power, and mode of each EV are independent of each other, the Monte Carlo sampling analysis method can be applied to generate random numbers using the stochastic probability distributions of EV driving conditions, battery characteristics, charging time, and charging modes. By doing so, the daily charging load curve for a single EV can be derived. The total charging load curve can be obtained by aggregating the charging load curves of each EV. The specific procedure is illustrated in Figure 3.

The method integrates factors such as daily mileage and capacity to consider the spatiotemporal distribution of electric vehicles. Employing Monte Carlo simulation and dynamic modeling technology, it accounts for the random nature of electric vehicle charging and discharging. The model captures the dynamic characteristics of the charging process by considering variability in charging power, battery capacity, and start time. This allows the model to simulate a daily charging load curve that reflects the different needs and behaviors of electric vehicles over time and in different locations. By considering the interaction between these factors and their time variation, the method can gain insight into the spatiotemporal characteristics of electric vehicle charging and discharging. The statistical model used by the method in this study can take into account the spatiotemporal characteristics by incorporating the relevant parameters and their variations, to understand the charging and discharging behavior of electric vehicles more comprehensively.

At the end of the process depicted in Figure 3, the convergence criterion is determined based on the stability of a statistical index, namely the variance coefficient, obtained from the Monte Carlo simulation. The variance coefficient is computed for the charging load curve and compared against a predefined threshold. When the variance coefficient falls

below the predefined threshold, it indicates that the simulation has converged to the desired level of accuracy. This convergence criterion ensures that the Monte Carlo simulation output achieves an acceptable level of precision in estimating the electric vehicle charging load. The variance coefficient is calculated according to Equation (5):

$$\varphi_t = \frac{\sqrt{V_t(\bar{L})}}{\bar{L}_t} = \frac{\sigma_t(\bar{L})}{\sqrt{N}\bar{L}_t} \tag{5}$$

where, φ_t is the variance coefficient of the charging load during t period, $t = 1, 2, \ldots 24$; $V_t(\bar{L})$ is the variance of the charging load during the t period; $\bar{L}_t$ is the expected value of charging load during t period; $\sigma_t(\bar{L})$ is the standard deviation of charging load during t period; N is the total number of electric vehicles and the number of simulations. When $\max(\varphi_t) < 0.05\%$, the simulation is convergent and the load calculation process is finished. If the simulation does not converge, it is transferred to the $i = 0$ step of the calculation process in Figure 3 to continue the calculation simulation of the charging load.

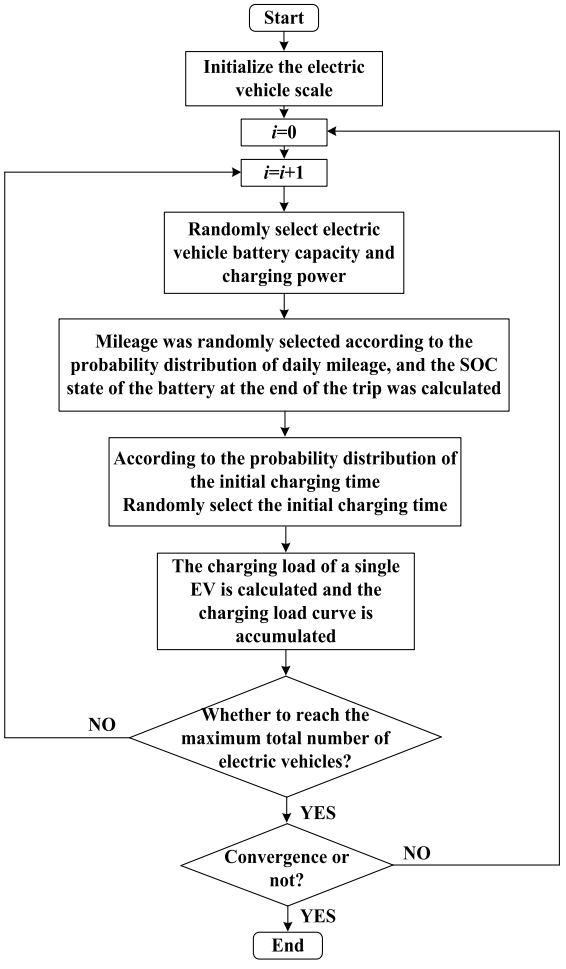

FIGURE 3. The calculation process of EV charging load based on Monte Carlo sampling.

In this study, different numbers of EVs were selected, and a Monte Carlo method was used for sampling analysis. It is important to note that the assumption is made that the grid does not guide or control the charging behavior of EVs. Hence, EVs can autonomously initiate charging upon connection to the grid. By employing a disordered random charging process, the total charging load curves for EVs of varying scales can be obtained, as shown in Figure 4. Additionally, the influence of disordered charging by EVs of different scales on the original load curve can be observed, as illustrated in Figure 5.

Based on the observed trends in Figure 4 and Figure 5, the charging load curve of electric vehicles exhibits distinct peak and valley characteristics over time. A large number of electric vehicles are charged between 16:00 and 24:00, resulting in the system load reaching its peak. Conversely, the charging demand is lowest between 5:00 and 10:00, which is closely associated with the lifestyle habits of the user population. The significant difference between the peak and valley values in the charging load curve of electric vehicles poses a challenge to the stable operation of the power grid. Without proper scheduling, it can lead to substantial power fluctuations in the system, impacting the normal operation of other electrical devices. It is necessary to include electric vehicles in optimization scheduling to reduce the impact on the power grid caused by their strong peak and valley characteristics during charging. The development of a rational charging optimization scheme becomes imperative to mitigate these negative impacts.

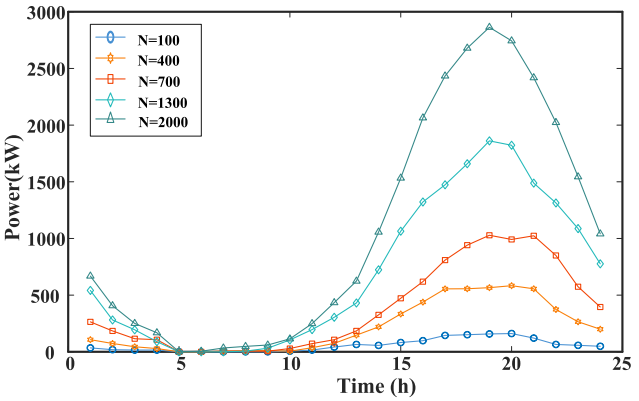

FIGURE 4. Charging load curves of different scale electric vehicles with unordered charging.

III. MULTI-OBJECTIVE OPTIMAL SCHEDULING MODEL OF ACTIVE DISTRIBUTION NETWORK

Based on the above analysis, this study aims to address the multiple challenges associated with electric vehicles charging in active distribution network. These challenges include "peak-to-peak" phenomena, cost reduction, smoothing of system load profile fluctuations, and improving the utilization of renewable energy. To achieve these objectives, this study primarily focuses on three main goals: minimizing operational costs, minimizing net load variations, and maximizing the utilization of photovoltaic energy. This study integrates multiple objectives into a unified framework for optimizing

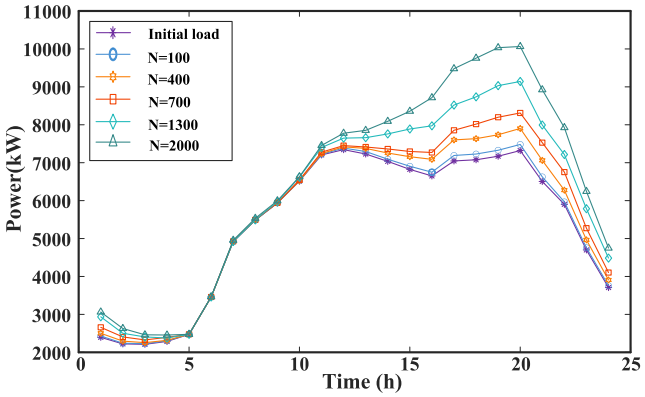

FIGURE 5. The influence of disordered charging of different scale electric vehicles on the initial load.

EV charging and grid stability. While individual objectives may have been considered separately in previous studies, their simultaneous optimization and investigation within the specific context of this research add novelty and value to the field.

A. OBJECTIVE FUNCTION

This paper proposes a multi-objective optimization approach for the operation of distribution network. The objective function, defined as Equation (6), comprises three sub-objectives. The first objective aims to minimize the operational cost, as described by Equation (7). The second objective focuses on minimizing the variance of the net load, as described by Equation (14). The third objective aims to maximize the consumption rate of the photovoltaic system, as described by Equation (16).

$$\min f = f_1 + f_2 - f_3 \tag{6}$$

(1) Optimization objective 1: Minimizing operational costs in distribution network optimization scheduling.

$$\min f_1 = C_{\text{ess}} + C_{\text{pv}} + C_{\text{MT}} + C_{\text{grid}} + C_{\text{loss}} \tag{7}$$

where, f_1 represents the operation cost of the optimal dispatching of the distribution network. It encompasses the sum of various components, namely the dispatching cost of energy storage equipment C_{ess}, the operation and maintenance cost of PV power generation equipment C_{pv}, the burning up cost of micro gas turbine units C_{MT}, the cost of purchasing electricity from the large power grid C_{grid}, and the network loss cost C_{loss} of the distribution network. The charge and discharge cost of energy storage generated by scheduling C_{ess} can be expressed as:

$$C_{\text{ess}} = \lambda_{\text{ess}} \sum_{t=1}^{T} \sum_{h=1}^{N_{\text{ess}}} (P_{h,t}^{\text{cha}} + P_{h,t}^{\text{dis}}) \tag{8}$$

where, T is the number of optimized time periods; N_{ess} is the number of energy storage devices; $P_{h,t}^{\text{cha}}$ and $P_{h,t}^{\text{dis}}$ are respectively the charging power and discharging power of the energy storage device h at time t; λ_{ess} is the energy storage scheduling cost per unit power.

The operation and maintenance cost of a PV power station in the process of power generation C_{pv} can be expressed as:

$$C_{\text{pv}} = \lambda_{\text{pv}} \sum_{t=1}^{T} \sum_{d=1}^{N_{\text{pv}}} P_{d,t}^{\text{pv}} \tag{9}$$

where, N_{pv} is the number of PV power generation equipment; $P_{d,t}^{\text{pv}}$ is the power generation power of PV power generation equipment d at time t; λ_{pv} is the maintenance cost coefficient of PV equipment.

The burnup cost generated by the micro combustion turbine unit in the process of power generation C_{MT} can be expressed as:

$$C_{\text{MT}} = \sum_{t=1}^{T} \sum_{l=1}^{N_{\text{MT}}} a_l + b_l P_{l,t}^{\text{MT}} + c_l (P_{l,t}^{\text{MT}})^2 \tag{10}$$

where, N_{MT} is the number of micro-gas turbines; $P_{l,t}^{\text{MT}}$ is the power generated by the microturbine l at time t; a_l, b_l and c_l are the constant term, primary term, and secondary term coefficients of the combustion characteristics of the microturbine l, respectively.

The charging cost mainly comes from the electricity purchase cost from the charging station to the power grid. The electricity purchase cost from the large power grid C_{grid} can be expressed as:

$$C_{\text{grid}} = \sum_{t=1}^{T} \omega_t P_t^{\text{grid}} \Delta_t \tag{11}$$

where, Δ_t represents the length of time period t; P_t^{grid} denotes the average power supplied by the distribution network at time t; ω_t signifies the price of electricity at time t.

The cost of distribution network loss caused by dispatching C_{loss} can be expressed as:

$$C_{\text{loss}} = \sum_{t=1}^{T} \omega_t P_t^{\text{loss}} \Delta_t \tag{12}$$

$$P_t^{\text{loss}} = \sum_{(i,j) \in E} (I_{ij,t})^2 r_{ij} \tag{13}$$

where, P_t^{loss} is the network loss of the distribution network system in time period t; E is line set; $I_{ij,t}$ is the current amplitude of branch ij in time period t; r_{ij} is the impedance value of branch ij.

(2) Optimization objective 2: Minimizing the variance of system net load. The regulation demands that the traditional power supply meet a requirement known as the net load, which represents the load remaining after deducting the new energy output from the total electricity load. Under the premise of maintaining the existing traditional load, the charging power of electric vehicles is optimized to minimize the net load variance of the system. The net load can determine the peak load demand of the generator, and the load mean square error is an index to measure the load fluctuation of the power grid, which can be used to quantify the stability

of the load change. The smaller the system net load variance, the more stable the load curve.

$$\min f_2 = \frac{1}{T}\sum_{t=1}^{T}(P_t^{\text{load}} + P_t^{\text{ev}} - P_t^{\text{pv}} - \overline{P})^2 \tag{14}$$

$$\overline{P} = \frac{1}{T}\sum_{t=1}^{T}(P_t^{\text{load}} + P_t^{\text{ev}} - P_t^{\text{pv}}) \tag{15}$$

where, f_2 represents the net load variance of the distribution network. P_t^{load} is the base load without considering EVs charging during the period t; P_t^{ev} is the total charging load of electric vehicles during the period t; P_t^{pv} is the output of the photovoltaic system during the period t; $P_t^{\text{load}} + P_t^{\text{ev}} - P_t^{\text{pv}}$ is the net load of the system; $\overline{P}$ is the average net load.

(3) Optimization objective 3: Maximizing the photovoltaic consumption rate. This objective aims to optimize and control the charging power of EVs in a way that maximizes the consumption rate of photovoltaic system without altering the traditional load.

$$\max f_3 = \frac{\sum_{t=1}^{T} P_t^{\text{pv}}}{\sum_{t=1}^{T} P_{t,\max}^{\text{pv}}} \times 100\% \tag{16}$$

where, f_3 represents the photovoltaic system consumption rate.

B. CONSTRAINTS

(1) System power balance constraint [23].

$$P_t^{\text{pv}} + P_t^{\text{MT}} + P_t^{\text{grid}} + P_t^{\text{dis}} - P_t^{\text{cha}} = P_t^{\text{load}} + P_t^{\text{ev}} + P_t^{\text{loss}} \tag{17}$$

System power balance constraints are essential considerations in power system optimization and operation. These constraints ensure that the total power supplied by generators matches the total power consumed by the loads, maintaining the stability and reliability of the system.

(2) The state constraints of charge and discharge of energy storage devices can be expressed as:

$$Y_{h,t}^{\text{cha}} P_{h,\min}^{\text{cha}} \le P_{h,t}^{\text{cha}} \le Y_{h,t}^{\text{cha}} P_{h,\max}^{\text{cha}} \tag{18}$$

$$Y_{h,t}^{\text{dis}} P_{h,\min}^{\text{dis}} \le P_{h,t}^{\text{dis}} \le Y_{h,t}^{\text{dis}} P_{h,\max}^{\text{dis}} \tag{19}$$

$$Y_{h,t}^{\text{cha}} + Y_{h,t}^{\text{dis}} \le 1 \tag{20}$$

$$E_{h,t}^{\text{ess}} = E_{h,t-1}^{\text{ess}} + (\eta_{\text{cha}}^{\text{ess}} P_{h,t}^{\text{cha}} - P_{h,t}^{\text{dis}}/\eta_{\text{dis}}^{\text{ess}})\Delta_t \tag{21}$$

$$0.2E_{h,\max}^{\text{ess}} \le E_{h,t}^{\text{ess}} \le 0.9E_{h,\max}^{\text{ess}} \tag{22}$$

$$\sum_{t=1}^{T}(\eta_{\text{cha}}^{\text{ess}} P_{h,t}^{\text{cha}} - P_{h,t}^{\text{dis}}/\eta_{\text{dis}}^{\text{ess}}) = 0 \tag{23}$$

where, $Y_{h,t}^{\text{cha}}$ and $Y_{h,t}^{\text{dis}}$ respectively represent the charge state and discharge state of the energy storage device h at time t; $P_{h,\min}^{\text{cha}}$ and $P_{h,\max}^{\text{cha}}$ are respectively the lower limit and upper limit of charge power of energy storage device h; $P_{h,\min}^{\text{dis}}$ and $P_{h,\max}^{\text{dis}}$ are respectively the lower limit and upper limit of discharge power of energy storage device h; $E_{h,t}^{\text{ess}}$ is the energy storage capacity of energy storage device h at time t; $\eta_{\text{cha}}^{\text{ess}}$ and $\eta_{\text{dis}}^{\text{ess}}$ are respectively the charge efficiency coefficient and discharge efficiency coefficient of the energy storage device; $E_{h,\max}^{\text{ess}}$ is the maximum energy storage capacity of energy storage device h.

(3) Electric vehicles charge power constraints.

$$0 \le P_t^{\text{ev}} \le N_{\text{ev}} P_{\max}^{\text{ev}} \tag{24}$$

$$E_t^{\text{ev}} = E_{t-1}^{\text{ev}} + \eta_{\text{cha}}^{\text{ev}} P_t^{\text{ev}} \Delta_t \tag{25}$$

$$E_{\min}^{\text{ev}} \le E_t^{\text{ev}} \le E_{\max}^{\text{ev}} \tag{26}$$

where, N_{ev} is the scale of electric vehicles; $P_{\max}^{\text{ev}}$ is the upper limit of charge power of electric vehicles; E_t^{ev} is the energy storage capacity of electric vehicles in the charging station at time t;$\eta_{\text{cha}}^{\text{ev}}$ is the charge efficiency coefficient of electric vehicles;$E_{\min}^{\text{ev}}$ and $E_{\max}^{\text{ev}}$ are respectively the minimum and maximum energy storage capacity of electric vehicles in the charging station.

(4) PV power constraint.

$$0 \le P_t^{\text{pv}} \le P_{t,\max}^{\text{pv}} \tag{27}$$

where, $P_{t,\max}^{\text{pv}}$ is the maximum output of PV power generation at time t.

(5) Micro-gas turbine power constraint.

$$P_{t,\min}^{\text{MT}} \le P_t^{\text{MT}} \le P_{t,\max}^{\text{MT}} \tag{28}$$

where, $P_{t,\min}^{\text{MT}}$ is the minimum output of micro-gas turbine power generation at time t; $P_{t,\max}^{\text{MT}}$ is the maximum output of micro-gas turbine power generation at time t.

(6) Safe operation constraints.

$$P_{i,t} = U_{i,t}\sum_{j=1}^{N} U_{j,t}(G_{ij}\cos\theta_{ij,t} + B_{ij}\sin\theta_{ij,t}) \tag{29}$$

$$Q_{i,t} = U_{i,t}\sum_{j=1}^{N} U_{j,t}(G_{ij}\sin\theta_{ij,t} - B_{ij}\cos\theta_{ij,t}) \tag{30}$$

$$U_{i,\min} \le U_{i,t} \le U_{i,\max} \tag{31}$$

where, N is the set of nodes; Equations (29) and (30) are nodal power flow constraints, and Equation (31) is nodal voltage constraint. $P_{i,t}$ and $Q_{i,t}$ are respectively the active and reactive power injected by node i at time t. $U_{i,t}$ and $U_{j,t}$ are the voltage amplitudes at nodes i and j at time t, while $\theta_{ij,t}$ is the phase angle difference between nodes i and j at time t. G_{ij} and B_{ij} are the conductance and susceptance of branch ij. $U_{i,\min}$ and $U_{i,\max}$ are the lower and upper voltage limits of node i, respectively.

(7) Line flow constraint: The line flow constraint plays an important role in ensuring the reliable and safe operation of the power system. By taking these limitations into account, we ensure that the power flowing through transmission lines does not exceed their capacity limits.

$$S_{ij}^{\min} \le S_{ij} \le S_{ij}^{\max} \tag{32}$$

where, S_{ij} is the power of branch ij; $S_{ij}^{\min}$ and $S_{ij}^{\max}$ are the lower limit and upper limit of the allowable transmission power between nodes i and j respectively.

The objectives of this model are to optimize the scheduling of equipment resources, such as energy storage system, PV system, micro-gas turbines, and electric vehicles, within the distribution network. The optimization aims to achieve the optimal comprehensive benefits of distribution network operation. Additionally, the model seeks to minimize the variance of the system net load and maximize the consumption rate of photovoltaic system.

IV. SOLUTION ALGORITHM BASED ON NSGAII-NDAX AND FUZZY THEORY

To achieve enhanced model scalability while minimizing the need for modifications to the power flow calculation matrices, this study has developed an integrated simulation and scheduling platform, as depicted in Figure 6.

MATPOWER [24] provides lower-level physical quasi-steady-state and dynamic simulation information, along with power flow calculation capabilities, within the MATLAB environment. MATLAB serves as the intermediate layer, responsible for constructing the optimization model, uploading power flow calculation results, and issuing control commands, among other tasks. The communication between these two layers is facilitated through API interfaces. At the top level, the multi-objective optimization model computation module interacts with the MATLAB intermediate layer via API interfaces, exchanging optimal solution sets, constraint functions, and other relevant information.

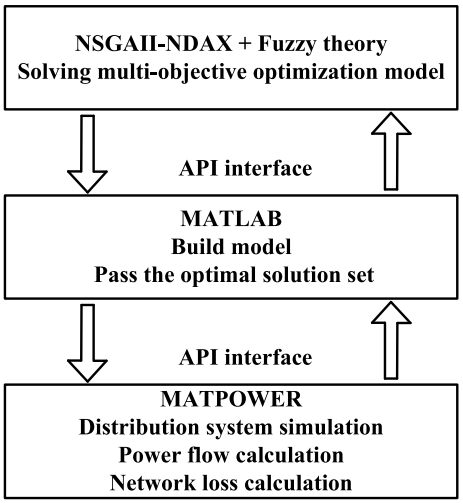

FIGURE 6. The framework of the co-simulation platform.

A. NSGAII-NDAX SOLUTION ALGORITHM

The proposed research model is a multi-objective nonlinear programming model with both equality and inequality constraints. It is challenging to solve the multi-objective problem by transforming it into a single-objective problem using appropriate weights. Therefore, this paper utilizes multi-objective algorithms to solve the aforementioned model. For multi-objective optimization problems, finding the global optimal solution is often challenging due to trade-offs between conflicting objectives. There exists a set of non-dominated solutions, known as the Pareto optimal solution set. The Pareto optimal solution set refers to the set of non-dominated solutions in multi-objective optimization problems. These solutions exhibit the characteristic that improving the performance of one objective requires compromising the performance of other objectives. By presenting the Pareto optimal solution set, this paper aims to allow decision-makers to explore a range of trade-off choices and make informed decisions based on their preferences. We propose an algorithm that combines an improved version of the Non-dominated Sorting Genetic Algorithm II (NSGAII) [25] algorithm with fuzzy theory, offering a flexible and robust framework for handling uncertainties and fuzziness in decision-making. This framework offers decision-makers a set of feasible alternative solutions, enabling them to make wise decisions based on their preferences and priorities.

The improved NSGAII incorporates an elite strategy in its evolutionary operations and utilizes the Simulated Binary Crossover (SBX) operator for an individual generation. The individual generation process is represented by Equation (33), where β is a random variable. However, due to the limited search range of β, the algorithm is prone to get trapped in local optima and may result in instability during the evolution process.

$$c_k^{1/2} = 0.5(y_k^1 + y_k^2) \pm 0.5\beta(y_k^1 - y_k^2) \tag{33}$$

where, y_k^1 and y_k^2 represent the two parent individuals of the kth generation obtained by crossover operation, and $c_k^{1/2}$ represents the two offspring individuals of the kth generation generated.

To address the limitations of the SBX operator and mitigate the issue of being trapped in local optima, a method called the Normal Distribution Adaptive Crossover (NDAX) operator has been proposed by [26] and [27]. The NDAX operator improves upon the standard normal distribution by incorporating a truncation operation and selecting a normal distribution function within the domain $(-T, +T)$ as a replacement for the random variable. The integral form of this normal distribution function is expressed as Equation (34).

$$\phi(x) = \int_{-T}^{T} \frac{1}{\sqrt{2\pi}} e^{-\frac{x^2}{2}} dx \tag{34}$$

The probability density function of the standard normal distribution is symmetric with respect to the Y-axis. From the symmetry, the following equation can be obtained:

$$\phi(x) = 2\int_{0}^{T} \frac{1}{\sqrt{2\pi}} e^{-\frac{x^2}{2}} dx = 2I \tag{35}$$

$$I^2 = (\int_{0}^{T} \frac{1}{\sqrt{2\pi}} e^{-\frac{x^2}{2}} dx)^2 = \frac{1}{\sqrt{2\pi}} \int \int_{0}^{T} e^{-\frac{x^2+y^2}{2}} dxdy \tag{36}$$

By introducing polar coordinates and setting $x = r\cos\theta$, $y = r\sin\theta$ and $\theta \in [0, \pi/2]$ into Equation (36), the following equation can be obtained:

$$I^2 = \int_0^{\frac{\pi}{2}} d\theta \int_0^T e^{-\frac{r^2}{2}} r dr = \frac{\pi}{2}(-e^{-\frac{r^2}{2}} + 1) \tag{37}$$

$$\phi(x) = 2I = 2\sqrt{\frac{\pi}{2}(-e^{-\frac{r^2}{2}} + 1)} \tag{38}$$

According to Equation (33), it can be deduced that when $0 \leq \beta \leq 1$, the genes of the offspring are located between the genes of the two parent individuals, while when $\beta > 1$, the genes of the offspring are located outside the genes of the two parent individuals. The probabilities of these two cases occurring are denoted as P_1 and P_2, respectively, and both are 0.5. The evolutionary process of the population is dynamic and not static. When individuals in the population tend towards local optima, efforts must be made to allow individuals to escape from local optima and expand the evolutionary space. In such cases, an adaptive population evolution strategy plays a crucial role.

In this study, we introduce the development rate P_1 and the expansion rate P_2. The P_1 represents the probability of using the crossover operator during population evolution, while the P_2 represents the probability of using the mutation operator. Depending on the different stages of population evolution, the selection of crossover and mutation operators also dynamically changes. In the initial stage of population evolution, a strong crossover strategy and a weak mutation strategy are adopted, while when the population evolves slowly and falls into local optima, a weak crossover strategy and a strong mutation strategy are employed. The aforementioned strategy adjustments contribute to enhancing the diversity of the population, thereby better exploring the solution space and overcoming the dilemma of falling into local optima.

The fitness values are mapped to the (0,1) probability interval, as shown in Equation (39).

$$\sigma = \frac{1}{1 + e^{\frac{-f_k^m}{10}}} f_k^m \tag{39}$$

where, σ is the *sigmoid* function; f_k^m is the fitness value of the individual m in the kth layer of the population, and let $\alpha = \sigma$ be the expansion rate adaptive parameter, which adaptively changes the crossover rate according to the individual fitness value in the population evolution. The expansion rate $P_2 = \alpha\varepsilon$, where ε is the expansion rate basis and the exploitation rate is $P_1 = 1 - P_2$, from which the following equation can be obtained:

$$2\sqrt{\frac{\pi}{2}(-e^{-\frac{r^2}{2}} + 1)} = \alpha\varepsilon \tag{40}$$

$$T = \sqrt{-\ln(1 - \frac{\alpha\varepsilon}{2\pi})} \tag{41}$$

Finally, the normal distribution adaptive crossover operator can be obtained as follows:

$$c_k^{1/2} = 0.5(y_k^1 + y_k^2) \pm 0.5\sqrt{-\ln(1 - \frac{\alpha\varepsilon}{2\pi})}(y_k^1 - y_k^2)\,|N(0,1)| \tag{42}$$

The objective of this study is to enhance the NSGAII algorithm by incorporating the NDAX operator. This operator is introduced to address the challenges associated with local optima and an unstable evolution process. Through the incorporation of the NDAX operator, the search range is expanded, ensuring that the Pareto-optimal solutions are uniformly distributed throughout the entire Pareto domain. This leads to increased diversity within the population and improves the quality of the Pareto optimal solutions obtained. Furthermore, the proposed algorithm is applied to the multi-objective optimization scheduling problems of integrating a large number of electric vehicles into an active distribution network. By utilizing this algorithm, decision-makers are provided with a larger number of representative non-dominated solutions, enabling them to make more rational decisions. This approach allows decision-makers to obtain a wide range of high-quality solutions, effectively balancing different objectives, and making decisions based on comprehensive considerations.

B. MECHANISM FOR EVALUATING PARETO OPTIMAL SOLUTIONS

In the process of using NSGAII-NDAX to solve the multi-objective optimization problem, a set of Pareto optimal solutions is generated. However, in practical grid operations, only one scheduling strategy can be implemented, requiring guidance for the operators. The size of the Pareto optimal solution set and the information diversity within the decision vectors pose challenges for operators in making well-informed decisions.

To address this issue, this study employs an optimal solution evaluation mechanism based on fuzzy mathematical theory and utilizing fuzzy membership functions, as constructed in [28]. This mechanism converts the degree of superiority or inferiority of each solution into fuzzy numerical values, providing decision support for the operators. Subsequently, we select the optimal scheduling solution from the Pareto front solution set to resolve this dilemma. This approach offers effective decision solutions for operators while retaining the significance of the original problem.

The single objective function value of each individual can be fuzzified according to the following membership function:

$$\mu_\xi^w = \begin{cases} 1 & F_\xi^w \leq F_\xi^{\min} \\ \dfrac{F_\xi^{\max} - F_\xi^w}{F_\xi^{\max} - F_\xi^{\min}} & F_\xi^{\min} \leq F_\xi^w \leq F_\xi^{\max} \\ 0 & F_\xi^w \geq F_\xi^{\max} \end{cases} \tag{43}$$

where, F_ξ^w is the wth front solution of the ξth objective; $F_\xi^{\min}$ and $F_\xi^{\max}$ respectively the minimum and maximum value of the front solution set of the ξth objective. μ_ξ^w represents the membership degree of the objective function after fuzzification, which indicates the closeness between the objective function value and the ideal value.

According to the max-min rule of fuzzy theory, the best scheduling scheme is selected. The specific expression

is as follows:

$$\mu^w = \min(\mu_1^w, \ldots, \mu_N^w);\ \forall w = 1, \ldots, k \qquad (44)$$

where, μ^w represents the membership function values for each scheduling scheme, while $\mu^{\max}$ represents the selection of the best scheduling scheme. The evaluation process in this study is based on the deviation between the objective function values and the desired values to determine the quality of the solutions. This method does not require the setting of weight coefficients to obtain the optimal scheduling scheme, demonstrating significant effectiveness in practical applications.

C. SOLUTION FLOW

The algorithmic flow of the proposed model-solving algorithm, which is based on the NSGAII-NDAX algorithm and fuzzy theory, is depicted in Figure 7.

The solution procedure can be outlined as follows:

Step 1: System initialization. Reading system line parameters, power parameters, loads data, EVs data, NSGAII-NDAX algorithm parameters, etc.

Step 2: Initialize the population G_g. According to the objective function equations (5) to (14), the control variables of the optimization model are vectors P_t^{pv}, $P_{1,t}^{\mathrm{MT}}$, $P_{2,t}^{\mathrm{MT}}$, …, $P_{l,t}^{\mathrm{MT}}$, P_t^{ess} and P_t^{ev}, if the step size is 1 hour, T=24, the $(l+3) \times 24$ dimensional population can be constructed to solve it, and a population of size N can be constructed as follows:

$$B_u = [P_1^{\mathrm{pv}}, \ldots P_T^{\mathrm{pv}}, P_{1,1}^{\mathrm{MT}}, \ldots P_{1,T}^{\mathrm{MT}}, \ldots P_{l,1}^{\mathrm{MT}}, \ldots P_{l,T}^{\mathrm{MT}}, P_1^{\mathrm{ess}}, \ldots P_T^{\mathrm{ess}}, P_1^{\mathrm{ev}}, \ldots P_T^{\mathrm{ev}}] \quad u = 0, 1, \ldots N-1 \qquad (45)$$

Step 3: Carry out the power flow calculation, calculate the fitness function value of each individual according to Equations (5) to (14), and calculate the fitness value of the population G_g.

Step 4: Perform non-dominated sorting on population G_g, calculate crowding degree, and screen out $N/2$ dominant individuals in the population as individuals of genetic variation.

Step 5: The offspring population is obtained by NDAX operator crossover and polynomial mutation for the selected dominant individuals H_g.

Step 6: Merge the current population G_g with the offspring population H_g to obtain population U_g. According to the fitness function value, recalculate the dominance relationship and crowding distance of each individual, and sort the individuals by Pareto.

Step 7: Keep the elite and select the first N individuals from population G_{g+1} as the parent population.

Step 8: Determine whether the maximum number of iterations is reached, if it is satisfied, the Pareto optimal solution set is obtained, otherwise return to step 4.

Step 9: The satisfaction degree of each Pareto solution is calculated by using fuzzy membership, and the optimization scheme with maximum satisfaction is obtained by comparison, which is the optimal compromise scheme of the power grid.

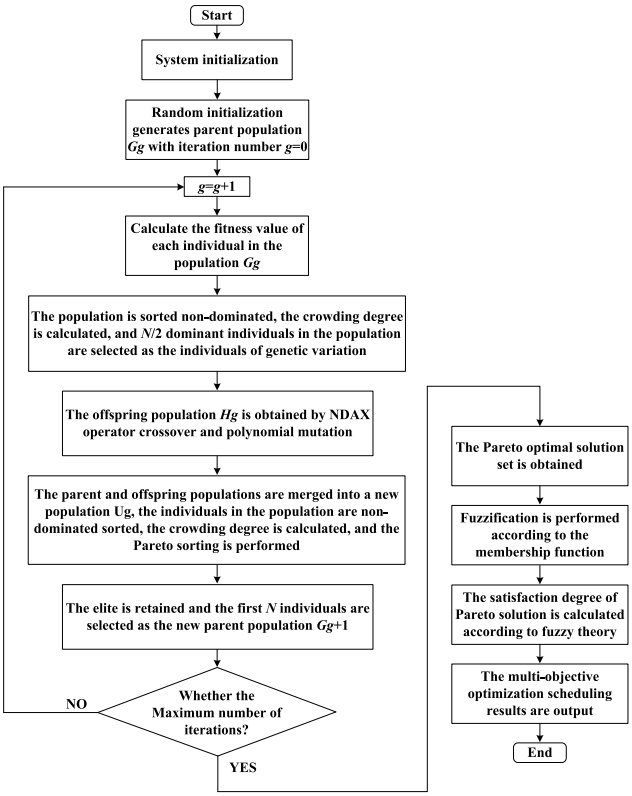

FIGURE 7. Solving process of multi-objective optimization model.

V. CASE ANALYSIS

A. CALCULATION PARAMETERS

In this case study, the improved IEEE 33-node distribution system [29] was utilized as the test case. The specific branch impedance and node load parameters adhered to the standard example. As depicted in Figure 8, a 2000 kW photovoltaic generation system was connected to node 6 of the distribution system. Additionally, three different models of micro-gas turbines with varying capacities were linked to nodes 20, 24, and 17, respectively, the MT parameters provided in Table 2. An energy storage system was connected to node 32, with the storage parameters provided in Table 3. Node 9 of the system was connected to an electric vehicle charging station, catering to a fleet of 400 electric vehicles.

The start and end times of electric vehicles trips follow normal distributions $N(7.32, 0.782^2)$ and $N(18.76, 1.30^2)$, respectively, and the daily travel distance follows a log-normal distribution $\log -N(3.66, 0.51^2)$. The battery capacities of the 400 electric vehicles follow a uniform distribution $U(20 \sim 30\mathrm{kW} * \mathrm{h})$, and the charge power follows a uniform distribution $U(4 \sim 6\mathrm{kW})$. The predicted daily power values for PV generation and loads in the system are shown in Figure 9. The parameters for market TOU pricing are presented in Table 4. The scheduling period is divided into one day intervals, resulting in a total of 24 time intervals for computation. In the MATLAB environment, we employ the NSGAII-DNAX algorithm to solve the problem. The population size is set to 100, the maximum number of iterations

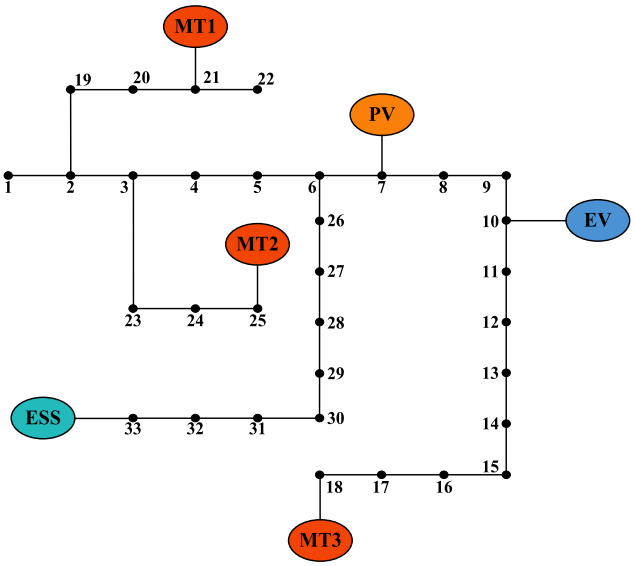

FIGURE 8. Improved IEEE33-node distribution network system.

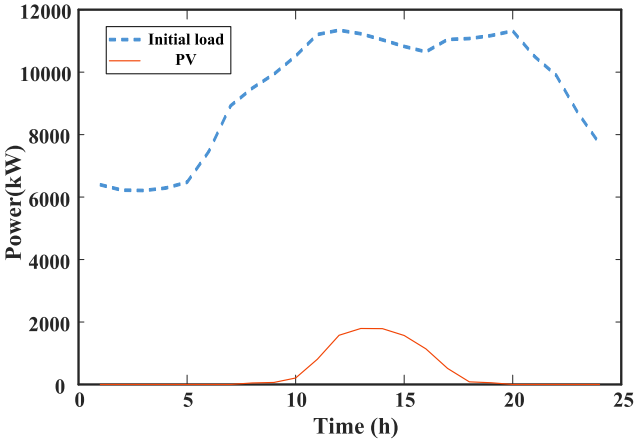

FIGURE 9. PV and load power prediction curve.

is 100, the expansion rate base value is 0.9, and the mutation rate is 0.1.

TABLE 2. Micro gas turbine parameters.

Unit	a [¥/(kW*h)^2]	b [¥/(kW*h)]	c (¥)	Lower limit (kW)	Upper limit (kW)
MT1	0.005	0.375	0	25	3000
MT2	0.005	0.435	0	25	3000
MT3	0.005	0.520	0	10	3000

TABLE 3. Energy storage parameter.

P^{cha}_{max} (kW)	P^{dis}_{max} (kW)	E^{ess}_{max} (kW*h)	SOC_{max}	SOC_{min}	η^{ess}_{cha}	λ_{ess} (¥ /kW)
600	550	4500	0.9	0.2	0.95	0.028

To explore the benefits of optimizing the scheduling of EVs charging power in terms of reducing distribution network operating costs, mitigating peak-to-valley load differences, and improving photovoltaic absorption rate, this study designs and compares three scheduling scenarios through simulation analysis. By analyzing these scenarios, we aim to gain insights into the effectiveness of various optimization strategies in achieving our research objectives.

TABLE 4. Time-of-use electricity price.

Periods.	The time periods.	Electricity price. (¥ /kW*h)
Peak period	10-12;18-22	0.993
Normal period	7-9;13-17;23-24	0.740
Valley period	1-6	0.497

Scenario 1: To establish a baseline reference for evaluating the effects of integrating electric vehicles into the distribution network, no electric vehicles are connected to the distribution network.

Scenario 2: 400 electric vehicles are connected to node 10 of the system via a charge station. The charging process is uncontrolled, meaning that electric vehicles start charging immediately upon arrival without any regulation or scheduling.

Scenario 3: 400 electric vehicles are connected to node 10 of the system via a charge station. The charging process follows the optimization scheduling scheme proposed in this study.

By conducting a comparative simulation analysis of these three scheduling scenarios, we can assess the impact of uncontrolled charging versus optimized scheduling on the system's performance.

B. SIMULATION RESULTS

Scenario 3 is solved by the NSGAII-DNAX algorithm, and the corresponding multi-objective Pareto front obtained by solving is shown in Figure 10. From Figure 10, it can be observed that the obtained optimal solutions are evenly distributed along the Pareto optimal front, effectively ensuring solution diversity. By further employing a fuzzy theory-based method for evaluation and analysis, the corresponding point in the figure represents the optimal compromise solution (f1=32064, f2=98.46%, f3=0.9543). The optimal generation scheduling scheme corresponding to the compromise solution can be found in Table 5 and is illustrated in Figure 11.

According to the data presented in Table 5 and Figure 11, during valley electricity price periods (e.g., 1:00-6:00 as shown in Figure 11), the generation cost of the three micro-gas turbines is higher than the cost of purchasing electricity from the grid. Therefore, the system primarily relies on the power grid to meet the load demand. However, during peak electricity price periods (e.g., 10:00-15:00 as shown in Figure 11), as the cost of purchasing electricity increases, the system significantly reduces the proportion of electricity purchased from the power grid, and the three micro-gas turbines become the main power supply units. At this time, the micro-gas turbines compete with each other based on

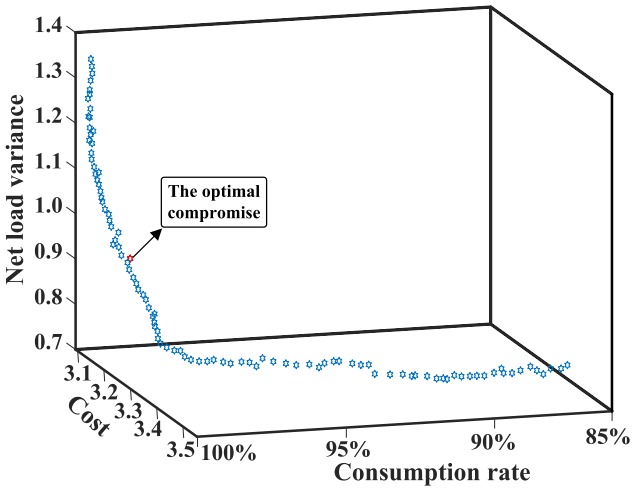

FIGURE 10. The Pareto optimal solution set corresponding to scenario 3.

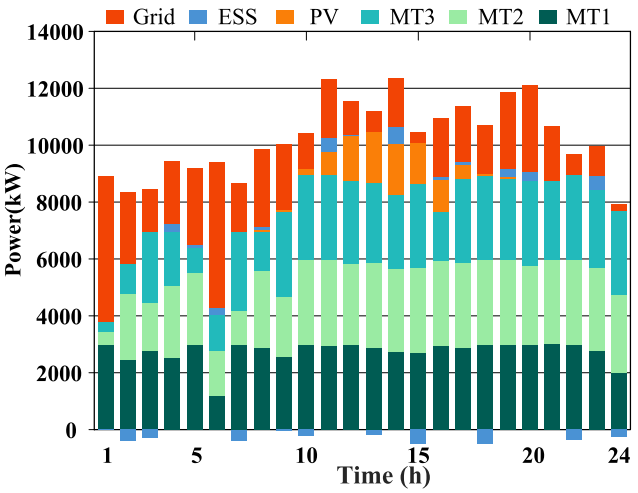

FIGURE 11. The optimal compromise solution corresponding to the generation schedule of power units.

TABLE 5. The scheduling scheme in scenario 3.

Time	MT1 (kW)	MT2 (kW)	MT3 (kW)	EV (kW)	ESS (kW)
1:00	2985.81	453.82	361.86	2005.25	-6.29
2:00	2453.25	2331.21	1043.72	2005.25	-409.16
3:00	2765.41	1683.34	2484.28	1987.44	-296.34
4:00	2519.42	2553.80	1874.21	2002.10	304.13
5:00	2996.33	2525.55	889.13	2003.69	87.77
6:00	1184.75	1583.68	1272.29	1146.14	241.46
7:00	2996.56	1206.07	2750.97	0	-382.51
8:00	2883.42	2705.13	1382.72	0	117.40
9:00	2574.40	2100.13	2971.27	0	-42.57
10:00	2997.62	2973.49	2999.04	0	-217.24
11:00	2972.16	2993.69	2994.30	0	491.67
12:00	2993.62	2839.17	2925.94	0	27.93
13:00	2875.33	2991.83	2806.73	0	-172.68
14:00	2733.63	2932.24	2581.78	0	586.30
15:00	2699.24	3000.00	2947.83	0	-511.88
16:00	2952.52	2998.93	1707.93	0	88.81
17:00	2887.63	2982.73	2936.06	0	102.39
18:00	2975.00	2992.06	2965.65	0	-505.73
19:00	2999.27	2976.40	2855.01	0	288.26
20:00	2998.59	2768.18	2986.55	0	330.41
21:00	2996.18	2982.99	2767.03	54.04	4.77
22:00	2999.27	2961.64	2992.90	32.92	-373.48
23:00	2768.21	2931.74	2716.40	88.02	521.91
24:00	1994.72	2738.46	2979.15	323.02	-275.25

their respective generation costs to determine their output levels. By implementing the proposed optimized operation and scheduling scheme, the system can significantly reduce its operating costs, resulting in an enhanced overall operational economy.

To validate the compliance of the system with network operational safety constraints during network operation, the analysis was conducted during a period of high charging load at time t=5 hour. Figure 12 illustrates the voltage distribution at each node. The results indicate that throughout the system operation, the voltage values at all nodes are distributed within the safe voltage range of 0.95 to 1.0 (per unit). This voltage distribution ensures the safety and reliability of the system, providing effective assurance for its normal operation.

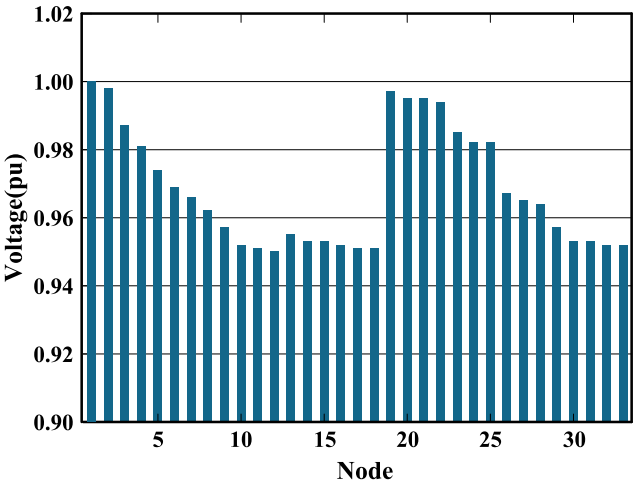

FIGURE 12. The voltage distribution at each node.

The load curves under the three scenarios are further compared, as shown in Figure 13. The corresponding load characteristic indicators are quantitatively compared through statistical calculations, as shown in Table 6.

TABLE 6. Load characteristic indices in different scenarios.

Scenario	Max load (kW)	Min load (kW)	Average load (kW)	Peak-valley ratio (%)
1	11344	6211	9401	45.25
2	12642	6290	9672	50.24
3	11344	8032	9886	29.19

Based on the observations from Figure 13 and the data presented in Table 6, it is evident that the uncontrolled charging strategy adopted by EVs in Scenario 2 leads to a

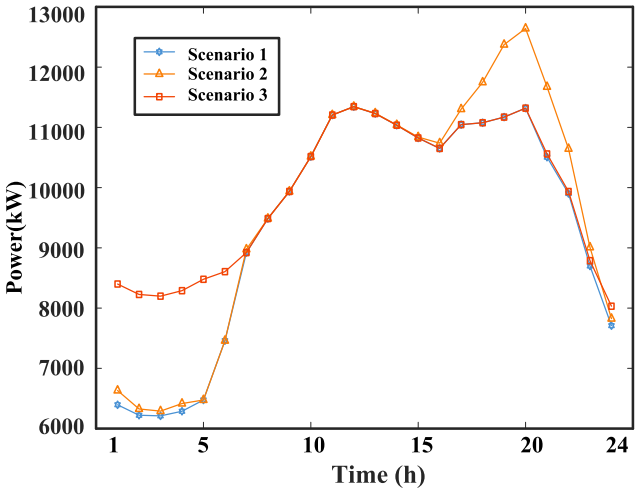

FIGURE 13. Comparison of load curves in different scenarios.

significant concentration of charging during the peak period of the evening load. Consequently, this results in a "peak-on-peak" load curve, causing the peak load to escalate from the original 11344 kW to 12642 kW. This approach not only increases the demand for peak shaving capacity, transformer, and substation expansion but also poses risks to the overall system operation safety.

However, the adoption of the optimized charging strategy in Scenario 3 markedly shifts the charging time toward the valley period of load, typically occurring from 1:00 a.m. to 6:00 a.m. By employing this optimization strategy, the load characteristics undergo a substantial improvement, reducing the peak-valley difference rate to 29.19% and increasing the load rate to 87.15%. Specifically, the optimized charging strategy achieves a 21.05% reduction in the peak-valley difference and a 10.65% increase in the load rate.

To further validate the advantages of the NSGAII-NDAX algorithm in active distribution network operation, we conducted a comprehensive comparison with several other algorithms, including the traditional NSGAII algorithm and those referenced in [30], [31], and [32]. The sub-objective function values of the obtained optimal solutions were statistically analyzed, and the convergence iteration count of the algorithm was recorded. By calculating the average values of these metrics, we conducted a comparative analysis of the optimal solutions and convergence iteration counts between the NSGAII-NDAX algorithm and the other algorithms, as shown in Figures 14-16 and summarized in Table 7.

Based on the data presented in Figures 14-16 and Table 7, a comparative analysis was conducted to evaluate the performance of the NSGAII-NDAX algorithm in optimizing the operation of active distribution systems. The following conclusions can be drawn:

The NSGAII-NDAX algorithm significantly reduced economic operational costs compared to the NSGAII algorithm and the algorithms presented in [30], [31], and [32]. The economic operational cost was reduced by 9.6% compared to NSGAII, 6.6% compared to [30], 6.7% compared to [31], and 3.1% compared to [32]. These findings indicate that the NSGAII-NDAX algorithm outperforms the other algorithms in terms of minimizing the overall cost of system operation.

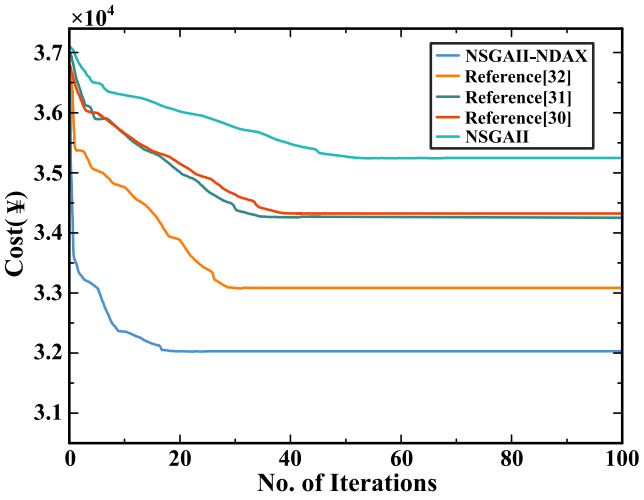

FIGURE 14. Convergence curve of operational costs.

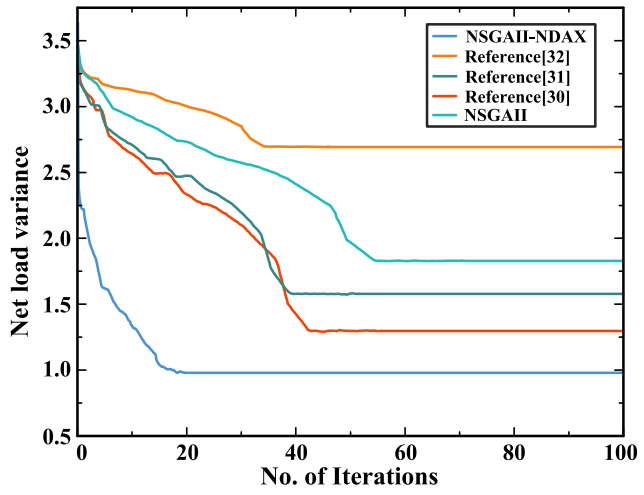

FIGURE 15. Convergence curve of net load variance.

The NSGAII-NDAX algorithm demonstrated superior performance in managing the net load variance of the system. It achieved a reduction of 46.9% compared to NSGAII, 26.4% compared to [30], 41.8% compared to [31], and 64.8% compared to [32]. These results highlight the effectiveness of the NSGAII-NDAX algorithm in mitigating fluctuations in power demand and supply, leading to a more reliable and efficient system operation.

The NSGAII-NDAX algorithm exhibited improved utilization of solar energy resources compared to the NSGAII algorithm and the algorithms in [30], [31], and [32].

It achieved an increase in PV consumption rate of 10.9% compared to NSGAII, 8.5% compared to [30], 19.1% compared to [31], and 2.3% compared to [32]. This indicates that the NSGAII-NDAX algorithm can effectively harness solar energy and promote the integration of renewable energy sources into the system.

The NSGAII-NDAX algorithm demonstrated faster convergence compared to the NSGAII algorithm and the algorithms in [30], [31], and [32]. It required fewer average convergence iterations to reach optimal solutions in a shorter timeframe. This characteristic enhances the timeliness and applicability of the NSGAII-NDAX algorithm, particularly in real-time or dynamic optimization scenarios.

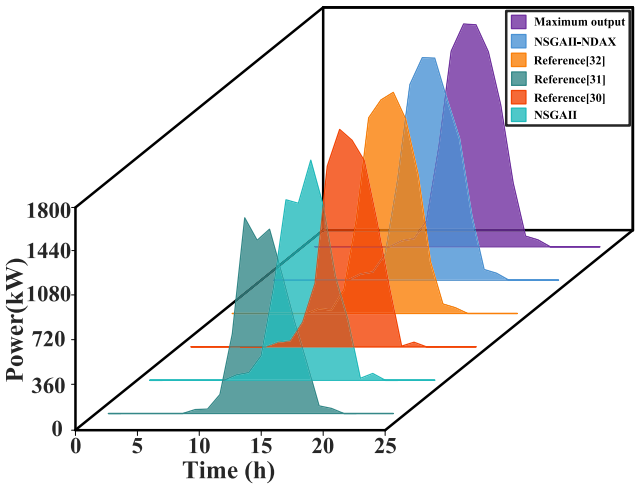

FIGURE 16. PV consumption levels for different algorithms.

TABLE 7. Algorithm comparison.

Algorithm	Cost (¥)	Net load variance	PV consumption rate (%)	Average convergence iteration count
NSGAII	35449	1.79	87.91	55
Reference [30]	34336	1.29	90.26	42
Reference [31]	34367	1.58	79.74	40
Reference [32]	33079	2.70	96.45	35
NSGAII-NDAX	32064	0.95	98.77	20

In summary, the comparative analysis emphasizes the superior optimization capabilities of the NSGAII-NDAX algorithm in comparison to the NSGAII algorithm and the algorithms presented in the references [30], [31], [32]. The NSGAII-NDAX algorithm exhibits a wider distribution of solutions, better convergence, stronger global search ability, improved economic performance, and faster convergence speed. These results demonstrate that the NSGAII-NDAX algorithm is highly suitable for optimizing the operation of active distribution systems, enabling efficient utilization of renewable energy resources, cost reduction, and alleviating fluctuations in system load.

VI. CONCLUSION

The optimization scheduling model for active distribution networks considering the large-scale integration of EVs is established in this paper. The optimization objectives of the model include minimizing the operational cost, reducing the variance of the net load, and maximizing the consumption rate of photovoltaic energy in active distribution networks. The NSGAII-NDAX algorithm is proposed to solve the optimization model. The results of case studies are as follows:

1) Optimizing the charging load of large-scale EVs and other controllable resources in active distribution networks can effectively improve the economic operation of the system, optimize the load curve, significantly reduce the peak-valley difference of the load, and enhance the consumption rate of photovoltaic energy.

2) The proposed NSGAII-NDAX algorithm exhibits characteristics such as a wider solution distribution, better convergence, stronger global search capability, improved economic efficiency, and faster convergence speed. It is highly suitable for the optimization operation of active distribution systems.

3) The combination of the NSGAII-NDAX algorithm and fuzzy theory-based evaluation method proposed in this paper addresses the challenges arising from the large size and rich information of the optimal solution set.

REFERENCES

[1] B. Duan, K. Xin, and Y. Zhong, "Optimal dispatching of electric vehicles based on smart contract and Internet of Things," *IEEE Access*, vol. 8, pp. 9630–9639, 2020.
[2] M. Ghavami, S. Essakiappan, and C. Singh, "A framework for reliability evaluation of electric vehicle charging stations," in *Proc. IEEE Power Energy Soc. Gen. Meeting (PESGM)*, Jul. 2016, pp. 1–5.
[3] E. Akhavan-Rezai, M. F. Shaaban, E. F. El-Saadany, and A. Zidan, "Uncoordinated charging impacts of electric vehicles on electric distribution grids: Normal and fast charging comparison," in *Proc. IEEE Power Energy Soc. Gen. Meeting*, Jul. 2012, pp. 1–7.
[4] M. Muratori, "Impact of uncoordinated plug-in electric vehicle charging on residential power demand," *Nature Energy*, vol. 3, no. 3, pp. 193–201, Jan. 2018.
[5] L. P. Fernandez, T. G. S. Roman, R. Cossent, C. M. Domingo, and P. Frias, "Assessment of the impact of plug-in electric vehicles on distribution networks," *IEEE Trans. Power Syst.*, vol. 26, no. 1, pp. 206–213, Feb. 2011.
[6] H.-l. Li, X.-m. Bai, and W. Tan, "Impacts of plug-in hybrid electric vehicles charging on distribution grid and smart charging," in *Proc. IEEE Int. Conf. Power Syst. Technol. (POWERCON)*, Oct. 2012, pp. 1–5.
[7] S. Deilami, A. S. Masoum, P. S. Moses, and M. A. S. Masoum, "Real-time coordination of plug-in electric vehicle charging in smart grids to minimize power losses and improve voltage profile," *IEEE Trans. Smart Grid*, vol. 2, no. 3, pp. 456–467, Sep. 2011.
[8] K. Clement-Nyns, E. Haesen, and J. Driesen, "The impact of charging plug-in hybrid electric vehicles on a residential distribution grid," *IEEE Trans. Power Syst.*, vol. 25, no. 1, pp. 371–380, Feb. 2010.
[9] M. R. Khalid, M. S. Alam, A. Sarwar, and M. S. J. Asghar, "A comprehensive review on electric vehicles charging infrastructures and their impacts on power-quality of the utility grid," *eTransportation*, vol. 1, Aug. 2019, Art. no. 100006.
[10] M. J. Rutherford and V. Yousefzadeh, "The impact of electric vehicle battery charging on distribution transformers," in *Proc. 26th Annu. IEEE Appl. Power Electron. Conf. Expo. (APEC)*, Mar. 2011, pp. 396–400.
[11] Z. Hu, Y. Song, Z. Xu, Z. Luo, K. Zhan, and L. Jia, "Impacts and utilization of electric vehicles integration into power systems," *Proc. CSEE*, vol. 32, no. 4, pp. 1–10, Feb. 2012.
[12] X. Zhu, H. Han, S. Gao, Q. Shi, H. Cui, and G. Zu, "A multi-stage optimization approach for active distribution network scheduling considering coordinated electrical vehicle charging strategy," *IEEE Access*, vol. 6, pp. 50117–50130, 2018.

[13] A. Chaouachi, E. Bompard, G. Fulli, M. Masera, M. D. Gennaro, and E. Paffumi, "Assessment framework for EV and PV synergies in emerging distribution systems," *Renew. Sustain. Energy Rev.*, vol. 55, pp. 719–728, Mar. 2016.
[14] A. Zakariazadeh, S. Jadid, and P. Siano, "Integrated operation of electric vehicles and renewable generation in a smart distribution system," *Energy Convers. Manage.*, vol. 89, pp. 99–110, Jan. 2015.
[15] S. Ge, L. Huang, and H. Liu, "Optimization of peak-valley TOU power price time-period in ordered charging mode of electric vehicle," *Power Syst. Prot. Control*, vol. 40, no. 10, pp. 1–5, May 2012.
[16] W. Tian, J. He, J. Jiang, L. Niu, and X. Wang, "Research on dispatching strategy for coordinated charging of electric vehicle battery swapping station," *Power Syst. Prot. Control*, vol. 40, no. 21, pp. 114–119, Nov. 2012.
[17] Q. Li, X. Xiao, J. Guo, and L. Lin, "Research on scheme for ordered charging of electric vehicles," *Power Syst. Technol.*, vol. 36, no. 12, pp. 32–38, Dec. 2012.
[18] E. Sortomme, M. M. Hindi, S. D. J. MacPherson, and S. S. Venkata, "Coordinated charging of plug-in hybrid electric vehicles to minimize distribution system losses," *IEEE Trans. Smart Grid*, vol. 2, no. 1, pp. 198–205, Mar. 2011.
[19] W. Shi, L. Lu, H. Gao, H. Li, Y. Liu, and J. Liu, "Economic dispatch of active distribution network with participation of demand response and electric vehicle," *Automat. Electr. Power Syst.*, vol. 44, no. 11, pp. 41–51, Apr. 2020.
[20] W. Yin and X. Qin, "Cooperative optimization strategy for large-scale electric vehicle charging and discharging," *Energy*, vol. 258, Nov. 2022, Art. no. 124969.
[21] K. Chaudhari, N. K. Kandasamy, A. Krishnan, A. Ukil, and H. B. Gooi, "Agent-based aggregated behavior modeling for electric vehicle charging load," *IEEE Trans. Ind. Informat.*, vol. 15, no. 2, pp. 856–868, Feb. 2019.
[22] L. Tian, S. Shi, and Z. Jia, "A statistical model for charging power demand of electric vehicles," *Power Syst. Technol.*, vol. 34, no. 11, pp. 126–130, Nov. 2010.
[23] Q. Kang, S. Feng, M. Zhou, A. C. Ammari, and K. Sedraoui, "Optimal load scheduling of plug-in hybrid electric vehicles via weight-aggregation multi-objective evolutionary algorithms," *IEEE Trans. Intell. Transp. Syst.*, vol. 18, no. 9, pp. 2557–2568, Sep. 2017.
[24] R. D. Zimmerman, C. E. Murillo-Sánchez, and R. J. Thomas, "MATPOWER: Steady-state operations, planning, and analysis tools for power systems research and education," *IEEE Trans. Power Syst.*, vol. 26, no. 1, pp. 12–19, Feb. 2011.
[25] S. Jeyadevi, S. Baskar, C. K. Babulal, and M. W. Iruthayarajan, "Solving multiobjective optimal reactive power dispatch using modified NSGA-II," *Int. J. Electr. Power Energy Syst.*, vol. 33, no. 2, pp. 219–228, Feb. 2011.
[26] H. Jiang, X. An, Y. Wang, J. Qin, and G. Qian, "Improved NSGA2 algorithm based multi-objective planning of power grid with wind farm considering power quality," *Proc. CSEE*, vol. 35, no. 21, pp. 5405–5411, Nov. 2015.
[27] D. Oz, "An improvement on the migrating birds optimization with a problem-specific neighboring function for the multi-objective task allocation problem," *Expert Syst. Appl.*, vol. 67, pp. 304–311, Jan. 2017.
[28] S. Nojavan, M. Majidi, A. Najafi-Ghalelou, M. Ghahramani, and K. Zare, "A cost-emission model for fuel cell/PV/battery hybrid energy system in the presence of demand response program: ε-constraint method and fuzzy satisfying approach," *Energy Convers. Manage.*, vol. 138, pp. 383–392, Apr. 2017.
[29] S. H. Dolatabadi, M. Ghorbanian, P. Siano, and N. D. Hatziargyriou, "An enhanced IEEE 33 bus benchmark test system for distribution system studies," *IEEE Trans. Power Syst.*, vol. 36, no. 3, pp. 2565–2572, May 2021.
[30] P. Shao, Z. Yang, Y. Guo, S. Zhao, and X. Zhu, "Multi-objective optimal scheduling of reserve capacity of electric vehicles based on user wishes," *Frontiers Energy Res.*, vol. 10, Oct. 2022, Art. no. 977013.
[31] L. Yang, W. Huang, C. Guo, D. Zhang, C. Xiang, L. Yang, and Q. Wang, "Multi-objective optimal scheduling for multi-renewable energy power system considering flexibility constraints," *Processes*, vol. 10, no. 7, p. 1401, Jul. 2022.
[32] X. Yang and G. Guo, "Source-load joint multi-objective optimal scheduling for promoting wind power, photovoltaic accommodation," *J. Renew. Sustain. Energy*, vol. 9, no. 6, Nov. 2017, Art. no. 065507.

JINGWEN CHEN was born in 1978. He received the Ph.D. degree in engineering from the Shaanxi University of Science and Technology, in 2020. He has been engaged in research on optimization and scheduling of electric vehicle charging loads, as well as microgrids and hybrid energy storage technologies. He has served as a Principal Investigator for one industrial research project in Shaanxi Province, one project funded by the Natural Science Foundation of Shaanxi Province, three projects from the Xi'an Science and Technology Bureau, one project from the Special Program of the Shaanxi Provincial Department of Education, and one project funded by the Doctoral Startup Foundation of Shaanxi University of Science and Technology. In addition, he has collaborated on 12 industry-academia cooperative projects. He has also participated in one project funded by the National Natural Science Foundation of China. He has been a key contributor to six provincial-level and municipal-level projects, as well as more than ten industry-sponsored projects.

LEI MAO was born in 1999. He received the bachelor's degree in electrical engineering and automation from the Shaanxi University of Science and Technology, where he is currently pursuing the master's degree in electrical engineering. His research interests include power system load forecasting and optimization of electric vehicle charging loads.

YAOXIAN LIU was born in 1990. He received the Ph.D. degree in electrical engineering from North China Electric Power University, in 2020. He has been engaged in research on demand response in new power systems, load forecasting, and non-intrusive load monitoring and decomposition.

JINFENG WANG was born in 1984. He received the Ph.D. degree. He is currently a Senior Engineer with the Energy and Development Research Center, State Grid Shaanxi Electric Power Company Ltd. Research Institute. He has been involved in research on demand-side management, demand response, and electricity market analysis.

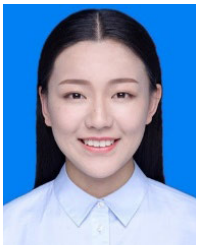

XIAOCHEN SUN was born in 1996. She received the master's degree. She is currently a Junior Engineer with the Energy and Development Research Center, State Grid Shaanxi Electric Power Company Ltd. Research Institute. She has been involved in research on demand-side management, demand response, and electricity market analysis.